



Delineation of recharge patterns and contaminant transport using ^3H – ^3He in a shallow aquifer contaminated by chlorinated solvents in South Korea

Dugin Kaown · Dong-Chan Koh · D. Kip Solomon · Yoon-Yeol Yoon · Jaeha Yang · Kang-Kun Lee

Abstract Stable isotopes of water and ^3H – ^3He were used to delineate recharge patterns and contaminant transport for a granitic regolith aquifer in an industrial complex in Wonju, South Korea, that has historically been contaminated with chlorinated solvents including trichloroethene (TCE) and carbon tetrachloride (CT). Groundwater recharge mainly occurred in upgradient forested areas while little recharge occurred in the downgradient industrial areas covered with extensive sections of impermeable pavement and paddy fields. $\delta^{18}\text{O}$ and δD data indicated that groundwater was mainly derived from summer precipitation. The apparent groundwater ages using ^3H – ^3He ranged from 1 to 4 yrs in the upgradient area and from 9 to 10 yrs in the downgradient area. Comparison of groundwater flow velocities based on Darcy's law and those calculated with simple mass balance models and groundwater age supported the presence of preferential pathways for TCE movement in the study area. Measureable TCE was observed in groundwater irrespective of groundwater age. Considering the 3-yr duration of the TCE spill, 14 yrs before sampling, this indicates that TCE plumes were continuously fed from sources in the

unsaturated zone after the spill ended and moved downgradient without significant degradation in the aquifer.

Keywords Environmental tracers · Recharge · Groundwater age · Chlorinated hydrocarbons · South Korea

Introduction

Chlorinated solvents are some of the most commonly detected contaminants in groundwater systems near industrial areas (Squillace et al. 2004; Rivett and Clark 2007). Chlorinated solvents are dense, non-aqueous-phase liquids (DNAPLs) that are more water soluble compared to common hydrocarbons, allowing them to more readily contaminate groundwater and surface waters with important consequences for human and environmental health (Sturchio et al. 1998; Beneteau et al. 1999; Shouakar-Stash et al. 2003). DNAPLs can migrate downward through the unsaturated and saturated zone due to their high specific gravity. Some of DNAPL-phase trichloroethene (TCE) will reach the water table, while part of the DNAPL mass is distributed to the residual phase in the unsaturated zone, since vertical movement is prevented by capillary trapping (Chambers et al. 2010; Luciano et al. 2010). The dissolved phase moves downgradient generating contaminant plumes. Understanding patterns of groundwater flow and contaminant transport within an aquifer are critical to control and to manage groundwater quality.

Information, especially related to age, describing groundwater flow and contaminant transport can be obtained using stable isotopes and environmental tracers. For example, groundwater age has provided useful information on sources and timing of recharge as well as on the vulnerability of aquifers to contamination (Böhlke and Denver 1995; Solomon et al. 1995; Manning et al. 2005; Morrison 2000; Gourcy et al. 2009; Kaown et al. 2009; Aeppli et al. 2010). Recharge rates determined by groundwater age and contaminant data were used in a simple mass balance model to determine the location of the contaminant source as well as the horizontal groundwater velocity (Solomon et al. 1995). ^3H – ^3He age

Received: 9 March 2013 / Accepted: 17 February 2014
Published online: 15 March 2014

© Springer-Verlag Berlin Heidelberg 2014

D. Kaown · J. Yang · K.-K. Lee
School of Earth and Environmental Sciences (BK21 SEES),
Seoul National University, Seoul, 151-747, Republic of Korea

D.-C. Koh (✉) · Y.-Y. Yoon
Korea Institute of Geoscience and Mineral Resources,
124 Gwahang-no, Yuseong-gu, Daejeon,
305-350, Republic of Korea
e-mail: chankoh@kigam.re.kr
Tel.: +82-42-868-3079
Fax: +82-42-868-3414

D.-C. Koh · Y.-Y. Yoon
University of Science and Technology,
217 Gajeong-ro Yuseong-gu, Daejeon,
305-333, Republic of Korea

D. K. Solomon
Department of Geology and Geophysics,
University of Utah, Salt Lake City, UT 84112, USA

dating was used to assess the susceptibility of public supply wells to contamination by volatile organic compounds (VOCs), pesticides, and nitrate (Manning et al. 2005). Environmental tracers and conceptual groundwater modeling have also been applied to assessments of groundwater flow and arsenic mobilization (Klump et al. 2006). Multiple tracers of tritium, chlorofluorocarbons (CFCs), and SF₆ have been applied to understand pesticide and nitrate transfer processes on a volcanic island (Gourcy et al. 2009). Finally, ³H–³He groundwater dating was used to verify numerical groundwater models in order to better define dissolved TCE transport and to guide the implementation of plume control systems in a deltaic sand aquifer (Murphy et al. 2011).

Some studies have focused on the relationship between DNAPL contamination and groundwater age (Aeppli et al. 2010; Murphy et al. 2011; Amaral et al. 2011). Before establishing plans for the treatment of the DNAPL source zones, detailed knowledge of the geochemical and hydrogeological characteristics, including groundwater flow, contaminant fate and transport mechanisms, must be obtained, because these factors can have great effect on treatment of the DNAPL sources.

The objectives in this study were to (1) evaluate the characteristics of groundwater flow and contaminant transport using environmental tracers and hydrogeochemical measurements, (2) determine the effects of those characteristics on the spatial distribution of dissolved chlorinated solvents in a shallow regolith aquifer in an industrial complex.

Study area

The site is on an industrial complex located approximately 75 km east of Seoul in South Korea, in an industrial area surrounded by low hills at the western border and by a stream in the northeastern part (Fig. 1a). The complex, which is about 1 km² in area, supports 40 public industrial, commercial, and residential buildings. Elevation in the study area ranges from 107–110 m above sea level (asl) in downgradient areas to 116–135 m in upgradient areas (Fig. 1b). The underlying aquifer consists of weathered and fractured Jurassic biotite granite overlain by soil and alluvial deposits of 10–15 m thickness (Yu et al. 2006; Baek and Lee 2011). The alluvial deposits consist primarily of two sediment types: silty sands and coarse sands. Hydraulic conductivity was measured by slug tests and was in the range of 2.0×10^{-4} – 2.4×10^{-3} cm/s in the alluvial material and 5.0×10^{-6} – 6.5×10^{-5} cm/s in the fractured granite. Water-table depth in the western portion of the study area ranges from 9 to 10 m in the summer and from 10 to 11 m in the winter, while water-table depth in the southeastern part of the study area ranges from 2 to 3 m in both summer and winter months. Seasonal variation in the west can be attributed to the fact that more than 66 % of the annual precipitation (about 1,359 mm/yr) is typically concentrated in the wet season (June–August) and less than 10 % in the dry season (November–January). The regional groundwater flow direction at this site is from west to east.

The western and eastern parts of the study area also display varying hydrogeology. First, the western portion is characterized by steep slopes while the eastern part is characterized by gently rolling slopes. Most of wells in the west are located within a weathered granite aquifer at greater depths (> 20 m) and are directly impacted by rainfall because most of the wells were constructed in unpaved areas. In contrast, wells in the eastern part of the study area are located within alluvial deposits with shallow well depths (< 20 m) and are not directly affected by rainfall because most of the area is covered by impermeable surfaces including asphalt and concrete. The aquifer in the downgradient area is heterogeneous and this area was used as paddy fields before the industrial complex was built in the 1970s (Baek and Lee 2011). Paddy fields in the upgradient areas are small scale and have poor spatial continuity; consequently, they are less effective to limit recharge. In contrast, paddy fields in the downgradient area were extensive and are now covered by pavement which could limit further recharge.

The Road Administrative Office of Gangwon Province used chlorinated solvents in the western portion of the study area to test pitch contents in asphalt, and dumped solvents without appropriate treatment of the waste solution (Gangwon Province 2005; Baek and Lee 2011). Carbon tetrachloride (CT) was first used for this test from 1982 to the 1990s. Then, TCE was employed after the Korean Ministry of the Environment regulated CT because of its potential health risks. The Road Administrative Office used 500 L of TCE annually and dumped the used TCE on the land surface surrounding the institute until 1997 (Yu et al. 2006). TCE concentrations exceeding South Korea's drinking-water standard of 30 µg/L were detected at two pumping wells owned by a local food company in July 1995 (Baek and Lee 2011). In 1999, TCE was detected at all pumping wells used by the food company, forcing the company to close those wells and to switch to the municipal water works. This incident led to a comprehensive investigation of the entire industrial area in order to elucidate the causes and sources of TCE contamination. Groundwater contamination with a mixture of chlorinated solvents such as trichloroethene (TCE) and carbon tetrachloride (CT) was observed in the study area.

Groundwater quality was monitored in Wonju for contamination by chlorinated solvents starting in November of 2009 and in March of 2010, and a high concentration of TCE was found in groundwater (7,260–11,300 µg/L in well KDPW-2; see Fig. 2) at the Road Administrative Office of Gangwon Province located in the western part of the study area (Yang and Lee 2012; Kaown et al. 2013). The TCE plume evidently moved 700 m downgradient toward the eastern area where TCE concentrations of 50–100 µg/L were found in 2010 (Fig. 2). The plume also moved northward as the result of heavy pumping in well PW-1 (~60 m³/day) from the less productive hard-rock aquifer, where a wet cleaning factory is located. Concentrations of CT during the study period ranged from 10 to 1,000 µg/L (Fig. 2), and the CT plume moved only as far as 400 m from TCE sources by 2010 (Yang and Lee 2012; Kaown et al. 2013).

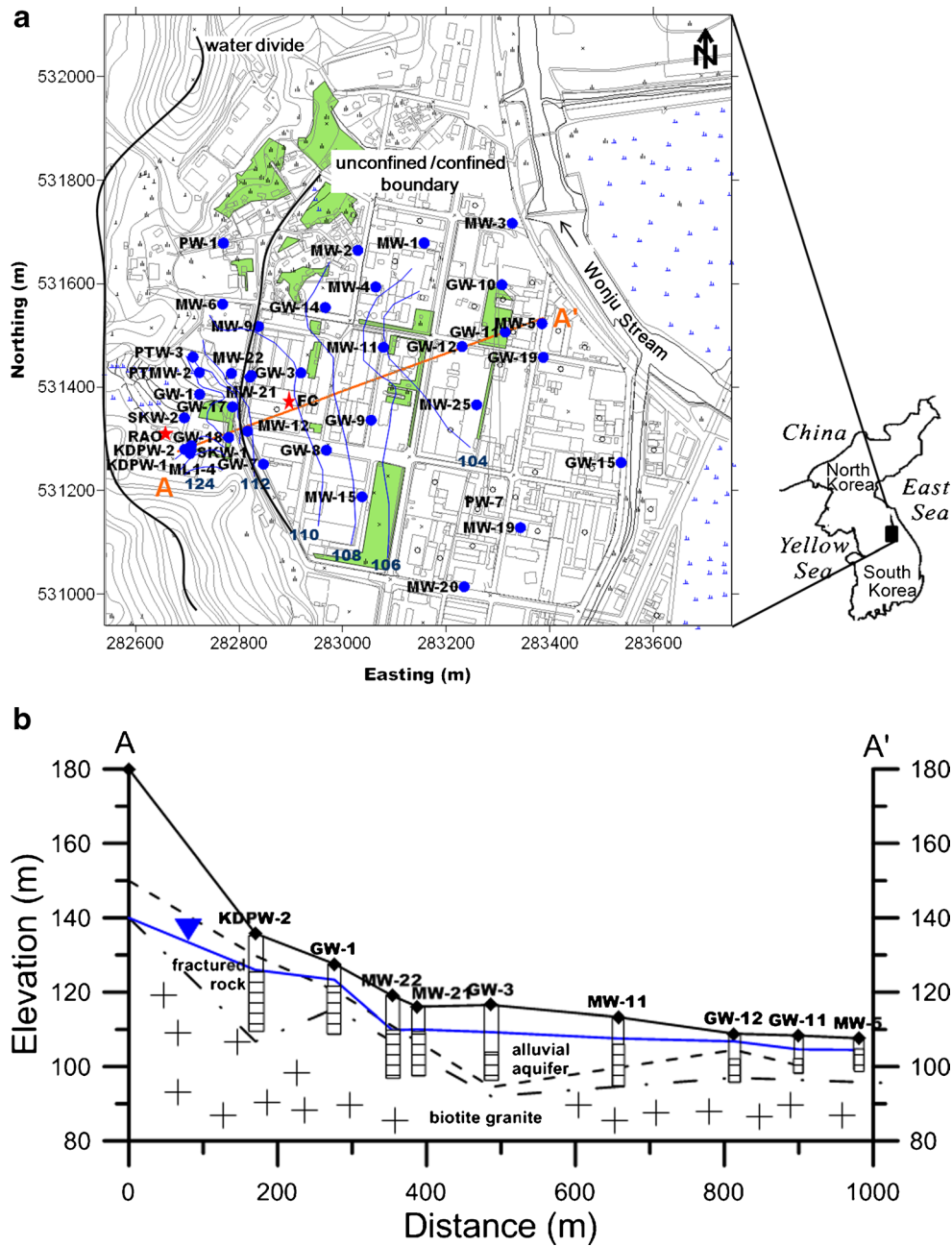


Fig. 1 a Location map of the Wonju site and the layout of the groundwater sampling wells (blue dots). Blue lines are contours of the measured water table—elevation, meters above sea level—for November 2009. The locations of the Road Administrative Office (RAO) and FC (a local food company where TCE was first detected) are indicated by red stars. The unpaved areas are shaded green. b Cross section A–A'. The blue, dashed, and dot-dashed lines indicate water table, a boundary between alluvial aquifer and fractured rock, and a boundary between fractured rock and biotite granite, respectively

Methods

Sampling

Between March and November of 2010, groundwater samples were collected using submersible and peristaltic pumps for chemical and isotopic analyses from 50 wells otherwise used for monitoring and industrial water supply (Fig. 1). Most of the wells were not used regularly after a municipal water supply was established in the area, with the exception of well PW-1 (Table 1).

The total depths of the wells ranged from 10 to 80 m, with most at depths between 10 and 30 m. The stable isotopes of water were analyzed to identify groundwater provenance and recharge pathways. Values for $\delta^{18}\text{O}$ and δD were measured with a VG PRISMII stable isotope ratio mass spectrometer at the Korea Basic Science Institute. Results were reported as δ notation relative to Vienna Standard Mean Ocean Water (V-SMOW) with a precision of $\pm 0.1\text{‰}$ for $\delta^{18}\text{O}$ and $\pm 1\text{‰}$ for δD (Lee and Lee 1999).

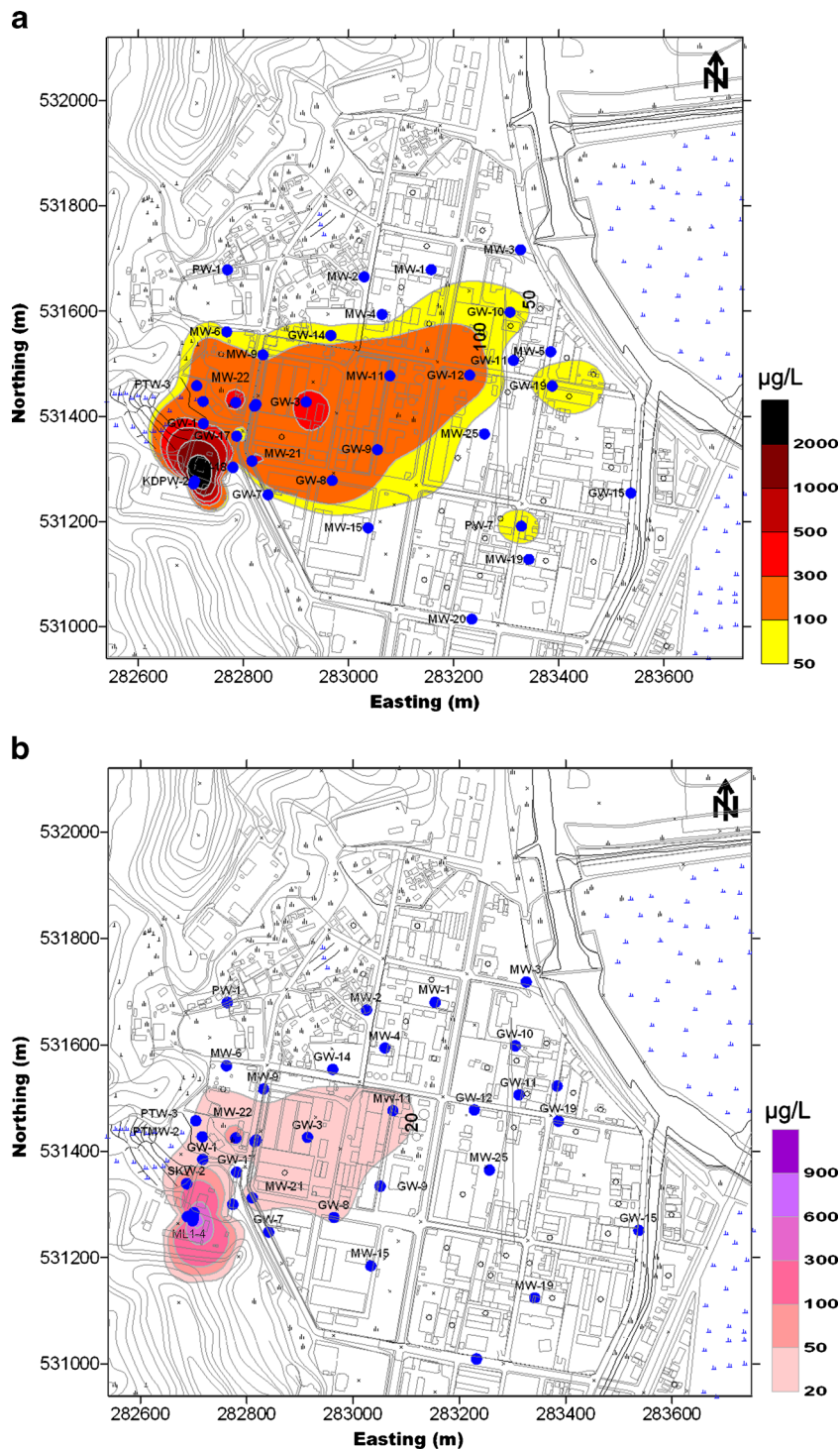


Fig. 2 Spatial distributions of a TCE and b CT concentrations in groundwater in samples obtained in March 2010. Blue dots are wells

Environmental tracers such as ^3H - ^3He , CFCs, and SF_6 can be applied to determine groundwater age and groundwater flow for the aquifer. In this study, the ^3H - ^3He method was expected to give better results than halocarbon-tracer-based methods since various chlorinated hydrocarbons may interfere with the measurement of CFCs either by co-elution on the chromatogram or through direct contamination of CFC-12, CFC-11 and Hydrogeology Journal (2014) 22: 1041–1054

CFC-113. Concentrations of noble gases were collected in copper tubes sealed at both ends with metal pinch clamps and were analyzed at the noble gas laboratories at the University of Utah, USA. The ^3He - ^4He ratio as well as ^4He , ^{20}Ne , ^{40}Ar , ^{83}Kr , and ^{131}Xe concentrations were determined with measurement errors of less than 1 % for ^3He - ^4He ratio and ^4He , 2 % for ^{20}Ne and ^{40}Ar , and 4 % for ^{83}Kr and ^{131}Xe . One-liter tritium samples were

Table 1 Specifications of the wells used for sampling in March 2010

Well No.	Elevation (masl)	Total depth (m)	Screened interval (m)	Depth to water (m)	Well use	Groundwater region
GW-3	117	25	14.5~25.0	7.3	M	D
GW-9	113	17	6.7~17.5	5.7	M	D
GW-10	109	14	8.3~14.3	4.6	M	D
GW-11	108	9	6.0~9.0	4.1	M	D
GW-12	109	19	8.0~18.3	2.5	M	D
GW-19	107	12	3.0~12.0	2.4	M	D
MW-1	108	16	5.5~16.0	1.7	M	D
MW-3	108	18	5.0~17.0	4.8	M	D
MW-4	110	26	7.0~26.5	3.6	M	D
MW-5	108	11	3.0~13.5	3.4	M	D
MW-11	113	19	6.0~19.5	6.0	M	D
MW-12	115	9	1.9~9.4	0.3	M	U
MW-21	116	18	5.5~18.0	6.1	M	U
PW-1	–	80	–	–	I	U
KDPW-1	136	50	30~50	10.8	M	U
KDPW-2	136	30	4.5~30	10.8	M	U
SKW-1	130	30	–	9.3	M	U
SKW-2	135	30	–	6.9	M	U
ML1-4	136	50	39.5~50	11.7	M	U
PTW3	124	24	6~24	9.4	M	U
PTMW2	124	50	27~50	8.5	M	U

M monitoring; *I* industrial; *U* upgradient; *D* downgradient

analyzed through the liquid-scintillation counting method at the Korea Institute of Geosciences and Mineral Resources with a detection limit of 0.6 TU (Yoon et al. 2007).

Models for dissolved noble gas

Three common models can be used to interpret dissolved noble gas concentration data in groundwater: (1) the unfractionated air model (UA model) that assumes the complete dissolution of entrapped air, (2) the partial re-equilibration model (PR model) that is based on the complete dissolution of entrapped air bubbles followed by diffusive degassing, and (3) the closed system equilibrium model (CE model) which assumes the incomplete dissolution of entrapped air (Aeschbach-Hertig et al. 2000). Calculated recharge temperatures generally range from lowest to highest in the following order of models: UA, CE, and PR. Since Xe solubility increases with decreasing temperature, calculated recharge temperatures tend to be higher for fractionation models compared to the UA model (Cey et al. 2008).

Results and discussion

Hydrogeochemistry

Hydrogeochemical data were plotted for major ions on a Piper diagram in Fig. 3. All groundwater samples were Ca-dominant, suggesting negligible signature of deep groundwater (> 100 m). Groundwater in the upgradient area can be divided into two groups depending on anion water type: (1) groundwater dominated by Cl^- and (2) groundwater with no dominant anion type. The Cl^- type groundwater showed higher concentrations of TCE compared to groundwater with no dominant type. Actually, the upgradient wells can be clearly distinguished by Cl^-

proportions. SKW-1, KDPW-2, SKW-2 and ML1-4 had higher Cl^- proportions and also had the highest TCE concentrations of 1–11 mg/L, while PTW-3, PW-1 and PTMW-2 had lower Cl^- and negligible TCE less than 200 $\mu\text{g/L}$. High concentrations of Cl^- in the upgradient area might be explained as the byproduct of the aerobic and anaerobic dechlorination of chlorinated solvents as well as the excessive input of NaCl from a soy sauce plant located in the upgradient area. The resulting clustered groups of groundwater types displayed different groundwater chemistries that were consistent with TCE concentration and the hydrogeological characteristics of the study area.

Concentrations of DO , NO_3^- , and SO_4^- were also monitored for 1 yr (Kaown et al. 2013). DO concentrations ranged from 0.2 to 5.8 mg/L in the study area. Most of the study area was under aerobic conditions, with the exception of the downgradient area, which was covered by impermeable pavement and was likely much less affected by rainfall. Partially anaerobic conditions in the downgradient area were also consistent with the fact that this area, located along a stream, was used for paddy fields before the industrial complex was built (Baek and Lee 2011). Concentrations of NO_3^- ranged from 0 to 1.7 mg/L in the downgradient area and from 12 to 24 mg/L in the upgradient area. Iron-reducing condition was observed in the downgradient area with a Fe^{2+} concentration that ranged from 0.1 to 3.3 mg/L compared to a concentration of less than 0.1 mg/L in the upgradient area. Concentrations of SO_4^- ranged from 6 to 76 mg/L, and a sulfate-reducing condition is unlikely to be observed in this study area. In summary, conditions in the upgradient area were primarily aerobic with high DO , while those of the downgradient area were generally anaerobic with lower DO and NO_3^- and higher iron concentrations. Thus, it is assumed that TCE was anaerobically degraded in the downgradient area.

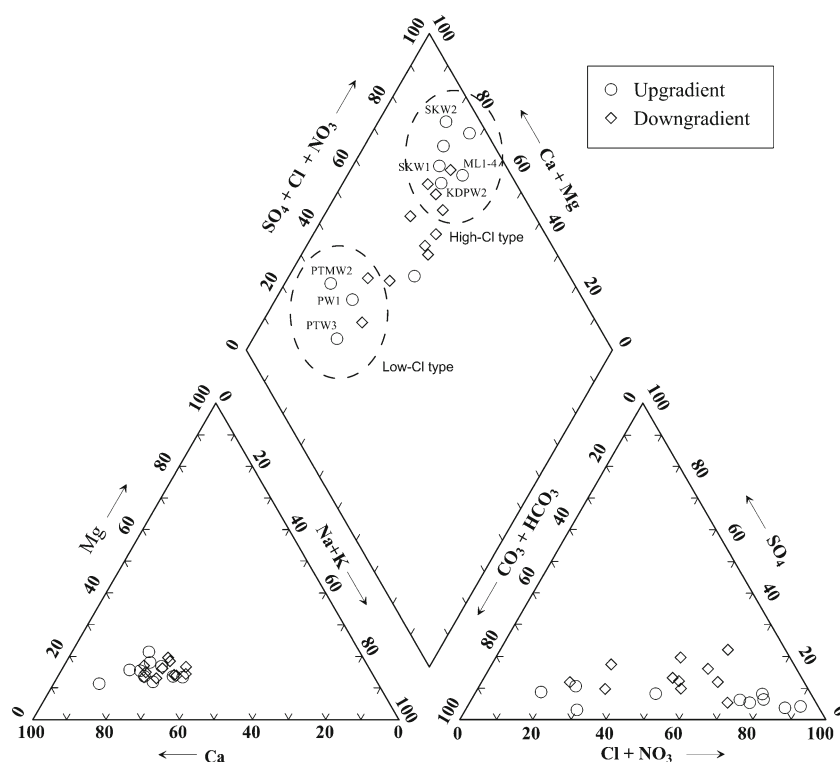


Fig. 3 Piper diagram for groundwater sampled in March 2010 (Kaown et al. 2013)

Stable isotopes of water

Values of δD and $\delta^{18}O$ in groundwater samples were compared with local meteoric water lines (LMWL) during both the wet and dry seasons, which were established by Lee and Lee (1999) for South Korea (Fig. 4). The isotopic composition of groundwater was congruent with that of the LMWL for the wet season, suggesting that most groundwater recharge occurred during the wet season when more than half of all precipitation occurred. In addition, stable isotopic signatures in many samples in the upgradient area were more enriched with δD and $\delta^{18}O$ and deviated downward from LMWL throughout the wet season. This is likely the result of infiltration of evaporated water from old paddy fields in the upgradient area (Koh et al. 2010).

Fractionation of dissolved noble gases

Dissolved noble gas concentrations (for Ne, Ar, Kr, and Xe) were fitted using the chi-square minimization method (Aeschbach-Hertig et al. 1999; Peeters et al. 2002) to obtain recharge temperature, amount of excess air, and degree of fractionation. The CE model had the lowest χ^2 for each of the samples, and all samples were significant ($p > 0.01$) with the exception of the sample from MW-4. Recharge temperature obtained by fitting noble gas data using the CE model (uncertainties < 2 °C) was 12.5 °C on average (Table 2), which was close to the mean annual air temperature (MAAT; 11.8 °C) at the nearby Wonju meteorological station during the period from 1996 to 2010 (Korea Meteorological Agency). In addition, recharge temperature was slightly lower than the measured

groundwater temperature (mean 14.2 °C) for corresponding samples.

Considerable portions of groundwater had significant terrigenous He which comprised up to 70 % of He when corrected for contribution of excess air (Fig. 5). The high terrigenous helium has been observed elsewhere in fractured granite in Korea (Lee et al. 2011; Jeong et al. 2012), which indicates $^3H-^3He$ ages are likely to be affected by terrigenous $^3He-^4He$ ratio (R_{terr}). R_{terr} was first assumed as the typical radiogenic value of 2×10^{-8} (Mamyrin and Tolstikhin 1984), considering that lithology of the study area is extensive and tectonically stable Jurassic granite. Because there is no reported radiogenic value of R_{terr} in the study area, the upper limit of R_{terr} was estimated as 6.3×10^{-8} from results of analysis for well MW1, with a considerable fraction of terrigenous He, assuming all He in MW-1 is radiogenic. This range of R_{terr} is similar to the ranges used by other studies for shallow groundwater in tectonically stable areas (Holocher et al. 2001; Burton et al. 2002). $^3H-^3He$ ages were presented based on both R_{terr} values, and the age errors due to choice of R_{terr} were comparable to those from analytical uncertainties. The wells in the upgradient area had lower radiogenic He compared to those in the downgradient area, and some of the upgradient wells had a deeper total depth, indicating lack of contribution from deeper groundwater with high radiogenic He (Fig. 6). Redox conditions changed from aerobic in the upgradient area to anaerobic in the downgradient area. The lower nitrate concentrations in the downgradient area are likely the result of denitrification. The amount of excess nitrogen from denitrification was estimated by comparing dissolved nitrogen

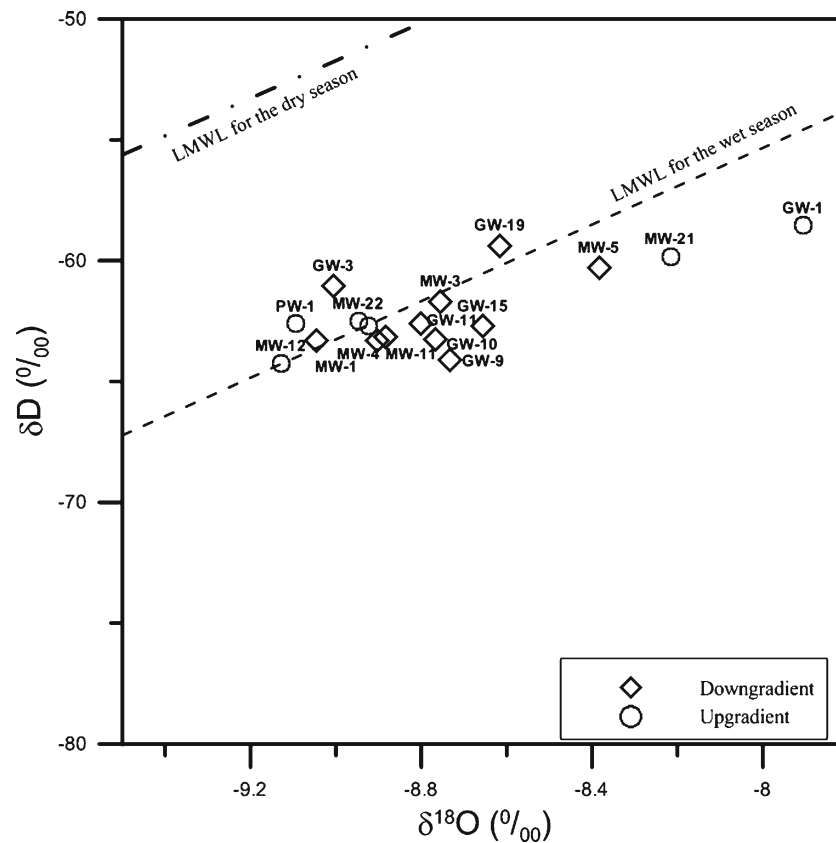


Fig. 4 Isotopic compositions of oxygen and hydrogen in groundwater samples

concentrations with those predicted by the CE model using Ne, Ar, Kr, and Xe measurements. Excess nitrogen was distinctively higher in the downgradient area compared to the upgradient area, suggesting active denitrification in the downgradient area (Fig. 7). This corroborates with the variation of hydrogeochemical parameters along groundwater flow paths.

³H–³He systematics

³H–³He groundwater ages were compared to the ³H precipitation input history to identify the effect of mixing pre-bomb groundwater recharged before the 1950s (Aeschbach-Hertig et al. 1998; Manning and Caine 2007). ³H in precipitation data reconstructed for Daejeon near the central part of South Korea by Koh and Chae (2008) were used for comparison. For the period between 2002 and 2010, ³H concentrations in precipitation in the Chuncheon area were used, which is located near the Wonju area, after recalculation of the precipitation-weighted mean in monthly measurements given in the reports of Korea Institute of Nuclear Safety (KINS 2010). The two series of ³H inputs conformed to each other without significant discontinuity in temporal trends (Fig. 8).

Using the reconstructed ³H input, model curves were created for ³H and initial ³H. Because wells used in this study had relatively long, screened intervals (Table 1), groundwater samples were likely to be mixtures of water of varying ages (Zuber 1986). In this regard, the

dispersion model (DM) was employed (Fig. 9). Most of the wells conformed to the DM with higher dispersion indicating effects of groundwater mixing, possibly due to long screened intervals. However, the degree of mixing could not be identified for the wells with younger ages because the DM was not sensitive to dispersion parameters in this age range.

Some groundwater samples from wells GW-9, GW-10, GW-12, and MW-4 had higher ³H levels. Several studies have shown that higher ³H levels are related to the retardation of ³H movement in the unsaturated zone. Zoellmann et al. (2001) showed that the highly variable ³H distribution in a permeable, fractured basalt aquifer was well simulated by ascribing low recharge to the area with low-permeability thick loess covers. In addition, Manning et al. (2005) reported that a portion of groundwater samples from the Quaternary sediment aquifer near Salt Lake City, Utah, had ³H levels higher than expected given the input history, which was explained by residence time of up to 10 yrs in the unsaturated zone. However, depths to water in the study area reported here were in the range of 2–5 m in the downgradient area where most of recharge occurs. The thin unsaturated zone is unlikely to significantly retard recharging water.

The samples with higher ³H values were located in the downgradient area where anaerobic conditions prevail. Distribution of redox-sensitive species and higher excess N₂ (Fig. 7) strongly indicate that denitrification is active in the area. Recently, tritiogenic ³He loss by degassing of N₂ produced from denitrification was shown to have a

Table 2 Measured concentrations of dissolved noble gases and apparent groundwater ages in March 2010

Well No.	Collection date	He _{tot} (x10 ⁻⁸)	N _{2,tot} (x10 ⁻²)	Ar _{tot} (x10 ⁻⁴)	Ne _{tot} (x10 ⁻⁷)	Kr _{tot} (x10 ⁻⁸)	Xe _{tot} (x10 ⁻⁸)	R/R _a	Temp (°C)	A ^b (cc/kg)	F ^c (-)	³ H (TU)	³ He _{nit} (TU)	³ He- ³ He age (R=2 x 10 ⁻⁸) (yrs)	³ H- ³ He age (R=6.3 x 10 ⁻⁸) (yrs)	error in ³ H- ³ He age (yrs)	³ He _{nit} (final) (TU)	No ³ He _{nit}
GW-3	2010-03-19	6.80	1.62	4.02	2.70	9.01	1.19	0.92	13.5	0.01	0.43	3.9	N/A	N/A	N/A	N/A	N/A	No ³ He _{nit}
GW-9	2010-03-19	14.00	2.92	4.71	3.00	9.96	1.29	0.58	15.1	0.07	0.58	9.9	5.1	6	1.2	4.6	4.6	No ³ He _{nit}
GW-10	2010-03-18	13.37	2.29	3.86	2.10	8.51	1.24	0.54	12.6	0.10	0.91	6.6	12.5	18	0.9	11.8	11.8	No ³ He _{nit}
GW-11	2010-03-18	7.53	2.46	3.87	2.13	9.39	1.29	0.73	10.0	0.00	0.00	4.8	3.2	8	3.6	2.9	2.9	No ³ He _{nit}
GW-12	2010-03-18	18.56	2.49	4.41	2.85	9.01	1.24	0.43	15.1	0.04	0.59	8.1	5.6	7	1.4	4.6	4.6	No ³ He _{nit}
GW-19	2010-03-18	5.65	2.52	3.84	2.14	9.17	1.25	0.91	11.1	0.01	0.84	4.8	1.2	4	2.7	1.1	1.1	No ³ He _{nit}
MW-1	2010-03-18	14.42	1.63	4.28	2.67	9.58	1.32	0.46	10.8	0.02	0.57	3.4	1.4	6	4.8	0.7	0.7	No ³ He _{nit}
MW-3	2010-03-18	7.62	2.42	3.84	2.12	8.43	1.19	0.74	14.0	0.13	0.89	5.2	3.6	9	2.5	3.4	3.4	No ³ He _{nit}
MW-5	2010-03-18	6.86	2.26	3.93	2.03	9.27	1.30	0.76	9.8	0.18	0.97	4.7	3.1	8	4	4	3	No ³ He _{nit}
MW-11	2010-03-19	13.16	2.60	4.56	2.69	9.63	1.25	0.53	16.6	0.15	0.67	5.4	2.6	7	6	6	2	No ³ He _{nit}
MW-12	2010-03-19	6.74	2.02	4.15	2.52	9.78	1.30	0.85	10.3	0.01	0.59	3.6	N/A	N/A	-	N/A	N/A	No ³ He _{nit}
MW-21	2010-03-19	5.17	1.85	4.12	2.22	9.37	1.33	0.98	11.0	0.13	0.88	4.5	N/A	N/A	-	N/A	N/A	No ³ He _{nit}
PW-1	2010-03-19	8.17	1.79	4.19	2.60	8.52	1.24	0.76	14.5	0.04	0.66	4.0	0.3	1	3	3	N/A	No ³ He _{nit}
KDPW1	2010-03-17	7.51	1.59	4.64	3.14	9.99	1.24	0.98	15.2	0.05	0.52	3.9	N/A	N/A	-	N/A	N/A	No ³ He _{nit}
KDPW2	2010-03-17	6.35	2.02	4.36	2.76	10.33	1.30	0.98	10.8	0.02	0.57	4.9	N/A	N/A	-	N/A	N/A	No ³ He _{nit}
SKW-1	2010-03-17	6.05	1.94	4.16	2.54	8.82	1.22	0.98	14.6	0.05	0.69	3.6	N/A	N/A	-	N/A	N/A	No ³ He _{nit}
SKW-2	2010-03-17	7.52	1.47	4.34	2.83	10.61	1.35	0.87	8.8	0.01	0.19	3.2	N/A	N/A	-	N/A	N/A	No ³ He _{nit}
ML1-4	2010-05-12	5.90	1.75	4.01	2.42	9.22	1.26	0.97	11.4	0.01	0.63	6.8	0.3	0.8	0.7	2.6	0.3	No ³ He _{nit}
PTW3	2010-05-12	5.44	2.67	4.30	2.42	9.95	1.35	1.03	10.6	0.06	0.79	5.2	0.4	1	2	2	0	No ³ He _{nit}
PTMW2	2010-05-12	11.51	1.57	4.22	2.61	9.35	1.28	0.63	11.9	0.02	0.63	5.0	5.8	14	1.8	5.3	5.3	No ³ He _{nit}

Noble gas concentrations are in ccSTP/g

^aR is ³He-⁴He of the water sample and R_a is ³He-⁴He of air (1.384x10⁻⁶)

^bVolume of excess air

^cFractionation parameter

N/A not available

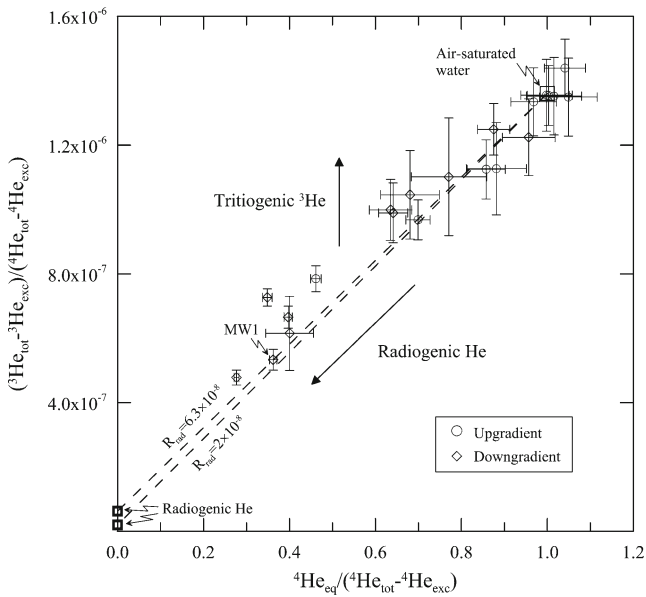


Fig. 5 Excess air-corrected ratio of ^3He - ^4He versus solubility equilibrium ^4He divided by excess air-corrected ^4He concentration. Each end member is dominated by two possible sources of He shown as an open diamond

significant effect on ^3H - ^3He age and a correction method using total dissolved gas pressure was developed by Visser et al. (2007, 2009) who showed that if exsolution of N_2 occurs below the water table overcoming hydrostatic pressure, dissolved noble gases partition into the gas phase and could be lost from the aquifer and/or during sampling. In this context, tritogenic ^3He may be lost during degassing due to excess N_2 for these samples, which significantly biased ^3H - ^3He age to younger ages, making the ^3H - ^3He relation deviate from DM models. However, only DM with the lowest dispersion parameter can account for higher ^3H values if ^3He was significantly

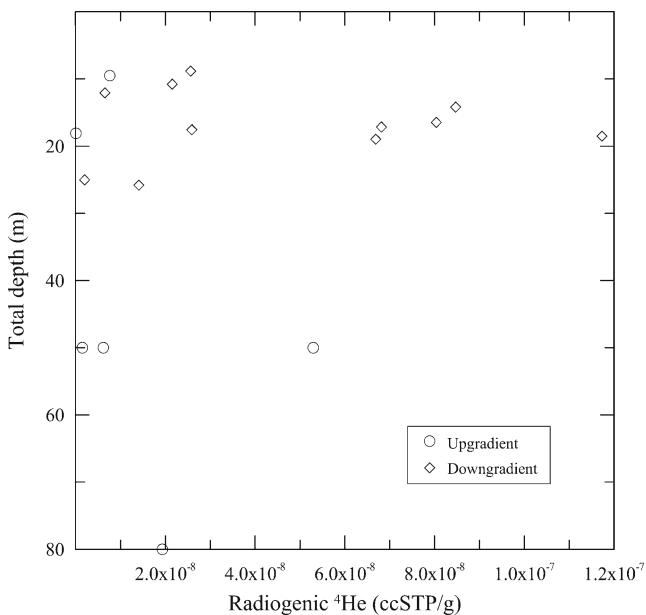


Fig. 6 Computed radiogenic He in groundwater versus total well depth

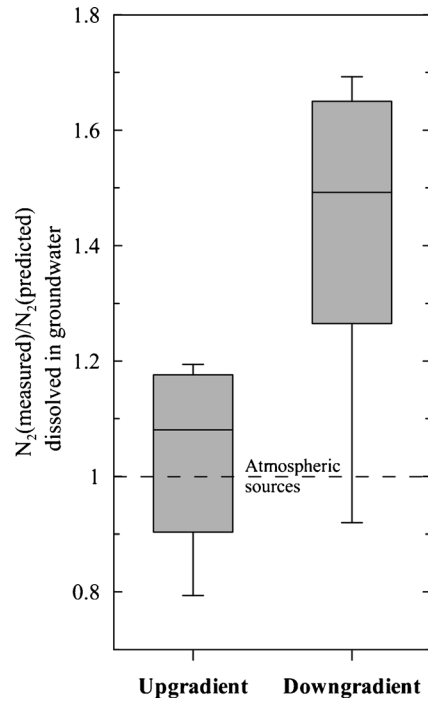


Fig. 7 Comparison of dissolved excess nitrogen from denitrification for the upgradient and downgradient areas. PTW3 was excluded from the upgradient group because it is located in a small paddy field

degassed, which is not plausible considering the relatively long-screened interval of the wells (Fig. 9). Also, other wells in anaerobic conditions including MW-5, GW-11, and GW-19 did not have higher ^3H values.

Shapiro et al. (1998) found a group of groundwater samples had ^3H values much higher than those expected from local precipitation in a buried-valley aquifer and suggested the elevated ^3H values could have resulted from the incinerator/landfill facility in the area. Manning et al.

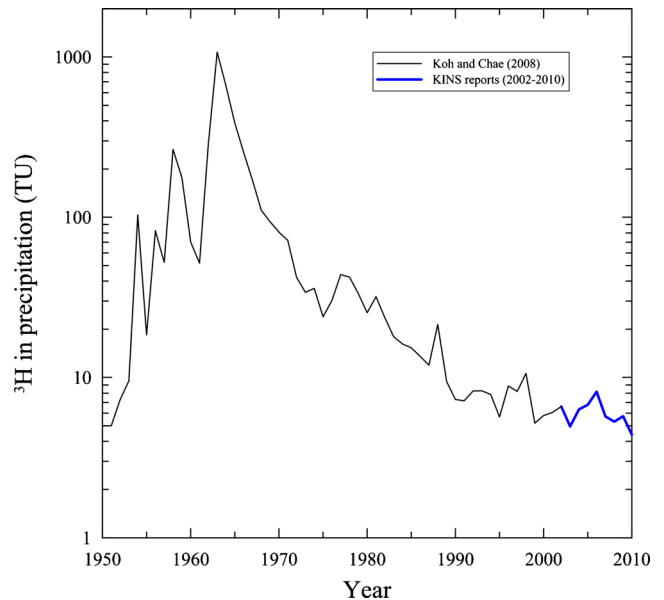


Fig. 8 Reconstructed ^3H input history for the site using two data sources of Koh and Chae (2008) and KINS reports (see text for further explanation)

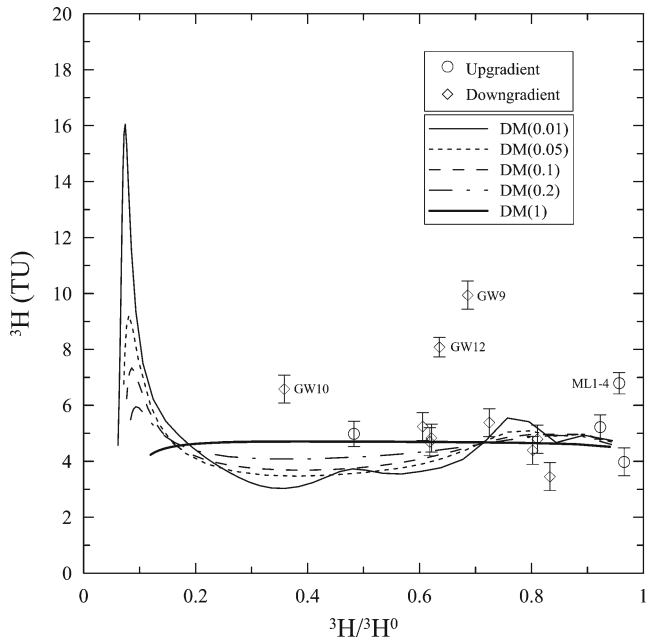


Fig. 9 Relation of initial tritium (measured ^3H + tritiogenic ^3He) and measured tritium concentrations based on the dispersion model, with dispersion parameters shown *in parenthesis*

(2005) argued these samples are affected by longer unsaturated zone residence time, though they also maintained that most of the samples had shorter (<5 yrs) unsaturated zone residence time, while not completely ruling out the possibility of ^3H contamination. Considering that various industrial facilities have been in operation

for decades in the Wonju study area, ^3H contamination from the local sources is more reasonable to explain the samples with higher ^3H values, though evidence for the local ^3H sources is not known.

Distribution of groundwater age

Groundwater ^3H values were in the range of 3–10 TU, illustrating that wells were dominated by recent recharge in the study area. The ^3H – ^3He ages of groundwater samples were determined by fitting results acquired from the CE model for dissolved noble gas and $R_{\text{rad}}=2\times 10^{-8}$, which estimated that groundwater ages were between <1 and 19 yrs, with the most probable range falling between 4 and 10 yrs. The range of groundwater ages seems to represent relatively fast groundwater flow through zones of weathered and highly fractured saprolitic granitic rocks (Fig. 1). Groundwater age was estimated as being between 1 and 4 yrs and between 9 and 19 yrs for the upgradient and downgradient portions of the study area, respectively (Fig. 10). However, groundwater age did not increase linearly from upgradient to downgradient areas and showed significant variability.

Wells ML1-4 and PW-1 in the upgradient area showed much younger groundwater age than that of PTMW2, which has similar total depth (50 m). This suggests that groundwater was composed primarily of recently infiltrated water, corresponding to the favorable hydrogeological characteristics for recharge in the upgradient area. In addition, the deepest well, PW-1, was also impacted by

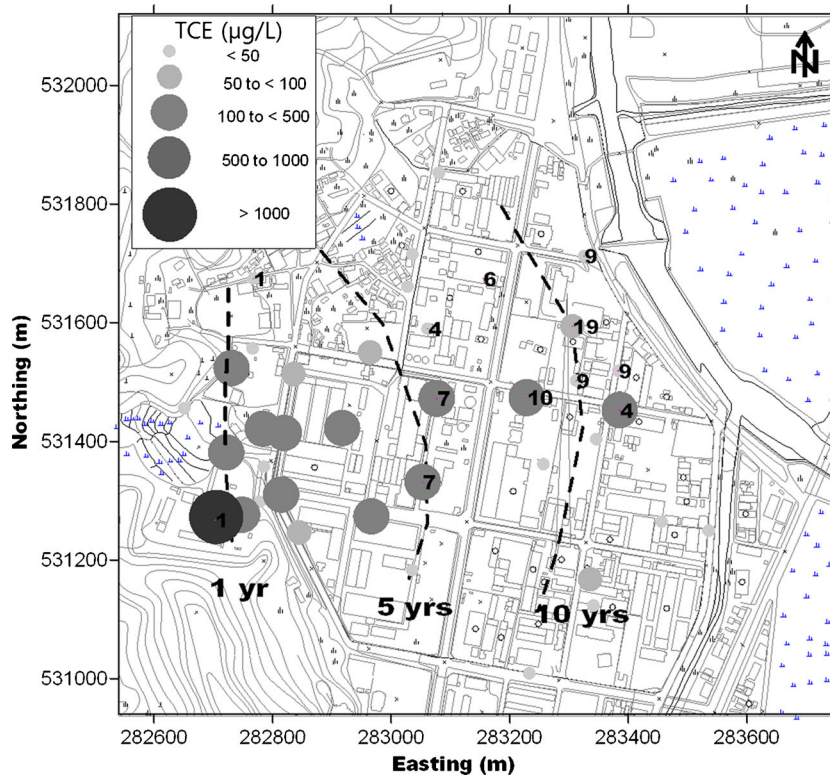


Fig. 10 Spatial distribution of TCE concentration (*circles*) and apparent groundwater age (contours: *dashed lines*) in the study area

heavy pumping which induced inflow from the upper weathered zone, as identified by Ayraud et al. (2008) at one of their study sites. Low concentrations of TCE in this well (Kaown et al. 2013) were detected, which could be attributed to pumping because this well was distant from the contaminant plume (Fig. 1).

Although the groundwater age for most wells in the downgradient area was estimated as being between 9 and 11 yrs (Fig. 10), some wells in the downgradient area displayed a wider range of estimated groundwater ages. GW-10 had a much older age (19 yrs), while GW-19 had a younger age (4 yrs). Groundwater older than 15 yrs is unlikely to contain TCE considering the TCE spill history assuming piston flow. Thus, GW-10 is likely to be a mixture composed of groundwater with ages less than 15 yrs and much older regional groundwater. This is related to the fact that the aquifer in the downgradient area is heterogeneous and that this area was used as paddy fields before the industrial complex was built in the 1970s (Baek and Lee 2011). Groundwater recharge in the area near GW-10 could be limited owing to low hydraulic conductivity in paddy fields, resulting in an older estimated age for groundwater. Well GW-19, on the other hand, had a depth to water that ranged from 1.7 to 2.4 m throughout the year (Table 1), which is shallower than most wells in the downgradient area. This may suggest that recharge was higher in the area near GW-19, resulting in younger groundwater compared to other wells in the area, which is supported by the dual ($\delta^{13}\text{C}$ and $\delta^{37}\text{Cl}$) isotope analysis results reported by Kaown et al. (2013). The TCE concentration and $\delta^{13}\text{C}$ values of TCE in GW-19 fluctuated during the year, which is most likely a reflection of mixing with fresh recharged water with dissolved material in the unsaturated zone.

Groundwater age and TCE spill history

High concentrations of TCE occurred in younger groundwater (estimated ages between 1 and 4 yrs) in the western, upgradient portion of the study area, and low-level TCE was observed in older groundwater (estimated ages between 9 and 19 yrs) in the downgradient area (Fig. 10). According to Gangwon Province (2005) and Baek and Lee (2011), TCE was assumed to be introduced to the subsurface between 1995 and 1997, which indicates that the spill event lasted for about 3 yrs, 14 yrs ago. TCE concentration was widely scattered over the entire range of estimated groundwater ages (1–19 yrs; Fig. 11). Taking a closer look at the distribution of TCE concentrations against estimated ages, two groups were identified: (1) group one had a relatively constant concentration of TCE, and (2) group two (the low-contamination group) had substantially lower TCE concentrations and was either located away from the direction of plume movement or at the distant margin of the plume (Fig. 1). When the low-contamination group was excluded from analysis, neither decreasing trend toward younger groundwater ages nor peaks near the TCE spill was found in terms of temporal variation of TCE concentration.

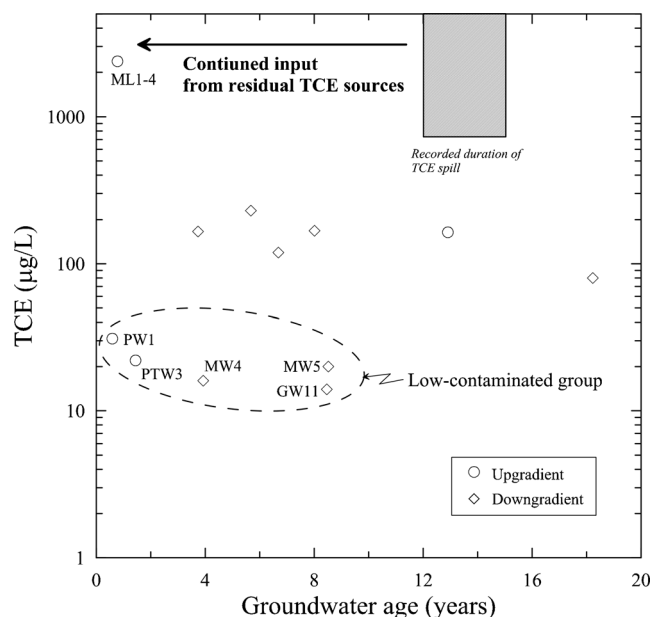


Fig. 11 Relation of TCE concentrations and apparent ages of groundwater. The duration of the TCE spill history is shown for comparison

This lack of trend can be explained by the fact that TCE was continuously released from the residual solvent plumes that resided at a depth within the unsaturated zone as well as saturated zone even after TCE was no longer actively used. This is consistent with the results by Yang and Lee (2012). They analyzed the influences of rainfall recharge events on the concentrations of the contaminants in groundwater and found multiple residual TCE sources in the unsaturated zone of the study area. In addition, it was also hypothesized that there was a high probability that preferential pathways for TCE movement existed along with recharge water because TCE concentration was already considerable in groundwater with ages close to the TCE spill history.

Groundwater flow velocities were calculated from two different kinds of data sets using (1) Darcy's law and (2) groundwater age. First, flow velocities (V) can be determined based on Darcy's law using hydraulic gradient (I), hydraulic conductivity (K) and effective porosity (θ) in the study area.

$$V = \frac{K \cdot I}{\theta} \quad (1)$$

When the hydraulic conductivity (K) is in the range of 2.0×10^{-4} – 2.4×10^{-3} cm/s in the alluvial material and 5.0×10^{-6} – 6.5×10^{-5} cm/s in the fractured granite, the hydraulic gradient (I) is 0.003–0.015, and the porosity (θ) is 0.1–0.3 in the study area (Park et al. 2011), the flow velocity in the study area would range from 9.8×10^{-6} to 1.2×10^{-4} cm/s (3–38 m/yr) in the upgradient area and from 1.9×10^{-6} to 2.1×10^{-5} cm/s (0.6–7 m/yr) in the downgradient area.

The flow velocity can be also estimated from the individual tracer-based apparent groundwater ages. In the study area, flow velocity was estimated using two limiting

cases of unconfined and confined aquifers since unpaved areas are mixed with paved areas where recharge is restricted. In an unconfined aquifer, the flow velocity can be determined using the following equations

$$V_x = \frac{x}{T} \cdot \ln\left(\frac{B}{B-z}\right) \quad (2)$$

where V_x is the horizontal velocity, x is the distance from the water divide along the groundwater flow direction (Fig 1a), B is the aquifer thickness, T is the travel time or groundwater age, and z is the depth below the water table (Solomon et al. 1995; Cook and Böhlke 2000). Homogeneous, unconfined aquifers of constant thickness receiving uniform recharge were assumed for Eq. (2). When the apparent groundwater age is about 0.8–19 yrs and the aquifer thickness is about 30–50 m in the study area, the estimated flow velocity in the unconfined aquifer would range from 54–234 m/yr in the upgradient area to 12–64 m/yr in the downgradient area (Table 3). The flow velocity in a confined aquifer can be estimated using the following equation:

$$V_x = \frac{x}{T} \cdot \ln\left(\frac{B}{B-z}\right) + \frac{x^*}{T} \quad (3)$$

where x is the distance from the water divide to the starting point of the confined aquifer, and x^* is the distance from the starting point of the confined aquifer to the sampling wells along the groundwater flow direction (Fig 1a; Cook and Böhlke 2000). The estimated flow velocity in the confined aquifer would range from 42 to 212 m/yr in the downgradient area. Based on results of two models, flow velocity in the study area was estimated to be from 12 to 234 m/yr. These values are faster than those based on Darcy's law by an order of magnitude. The discrepancy between the velocity values suggests that effective porosity is likely lower than assumed due to

preferential flow paths, which can explain the considerable amount of TCE in groundwater with ages corresponding to the recorded TCE spill history; the TCE is likely to move through the preferential pathways.

Summary and conclusions

Environmental tracers, including stable isotopes of water and ^3H - ^3He and hydrogeochemical parameters, in groundwater were employed to evaluate patterns of groundwater flow and contaminant transport in the aquifer systems of the study site. Stable isotopes of water indicated that groundwater recharge in that area occurred mainly through summer precipitation, which is more pronounced in the upgradient area. Evaporation signatures were found in some wells in the downgradient area, indicating infiltration from paddy fields. The estimated groundwater ages from ^3H - ^3He data (with corrections for excess air fractionation using dissolved noble gases) ranged from 1 to 19 yrs with the most probable range occurring between 4 and 10 yrs. Groundwater ages were between 1 and 4 yrs in the upgradient area and between 9 and 10 yrs in the downgradient area. The older age of groundwater in the downgradient area is congruent with the fact that groundwater recharge was limited there because of the prevalence of impermeable surfaces.

Finally, groundwater concentrations of TCE were relatively constant with no discernible temporal peaks compared to groundwater ages. Considering the 3-yr duration of the TCE spill 14 yrs before sampling, it is likely that TCE was continuously released, without any significant degradation, into the aquifer from residual sources in the unsaturated zone within the upgradient area even after the TCE spill ended. Flow velocity using groundwater age was estimated in two limiting cases of unconfined and confined aquifers and compared to Darcian velocity, which supported the preferential

Table 3 Groundwater flow velocity determined from the apparent groundwater ages

Well No.	Groundwater region	T (yrs)	Z (m)	x (unconfined) (m)	V_x (unconfined) (m/yr)		x (confined) (m)	x^* (m)	V_x (confined) (m/yr)	
					$B=30$ m	$B=50$ m			$B=30$ m	$B=50$ m
M11-4	U	0.8	20	170	233.5	108.6				
PW-1	U	1	20	200	219.7	102.2				
PTW3	U	1	15	150	104.0	53.5				
GW-9	D	7	12.7	570	44.8	23.9	300	270	83.4	62.4
GW-10	D	19	11.3	870	21.6	11.7	300	570	51.6	41.7
GW-11	D	9	7.5	870	27.8	15.7	300	570	91.1	79.0
GW-12	D	9	13.1	820	52.3	27.7	300	520	110.1	85.5
GW-19	D	4	7.5	890	64.0	36.2	300	590	211.5	183.7
MW-1	D	6	10.5	820	58.9	32.2	300	520	145.5	118.9
MW-3	D	9	11	890	45.2	24.6	300	590	110.7	90.1
MW-5	D	9	8.5	890	32.9	18.4	300	590	98.5	84.0
MW-11	D	7	12.5	600	46.2	24.7	300	300	89.1	67.5

U upgradient; D downgradient; T travel time or groundwater age; Z aquifer thickness; B depth below the water table; x distance from the water divide; V_x horizontal groundwater velocity; x^* distance from the starting point of the confined aquifer to the sampling wells

pathways for TCE movement in the study area. The results provided critical insights into the timing of groundwater flow and contaminant transport in both the unsaturated and saturated zones, and this information can be applied to establish more realistic and viable remediation plans in the study area.

Acknowledgements The thoughtful and valuable comments of Dr. John Karl Böhlke (USGS) are gratefully acknowledged. This work was supported by the Basic Research Project (14-3211-2) of the Korea Institute of Geoscience and Mineral Resources (KIGAM) funded by the Ministry of Science, ICT and Future Planning, the National Research Foundation of Korea Grant funded by the Korean Government [NRF- 2012R1A1A3013672] and ‘The GAIA Project (173-092-009)’ by the Korea Ministry of Environment.

References

- Aeppli C, Hofstetter T, Amaral HI, Kipfer R, Schwarzenbach R, Berg M (2010) Quantifying in situ transformation rates of chlorinated ethenes by combining compound-specific stable isotope analysis, groundwater dating, and carbon isotope mass balances. *Environ Sci Technol* 44:3705–3711
- Aeschbach-Hertig W, Schlosser P, Stute M, Simpson HJ, Ludin A, Clark JF (1998) A $^3\text{H}/^3\text{He}$ study of ground water flow in a fractured bedrock aquifer. *Ground Water* 36:661–670
- Aeschbach-Hertig W, Peeters F, Beyerle U, Kipfer R (1999) Interpretation of dissolved atmospheric noble gases in natural waters. *Water Resour Res* 35:2779–2792
- Aeschbach-Hertig W, Peeters F, Beyerle U, Kipfer R (2000) Palaeotemperature reconstruction from noble gases in groundwater taking into account equilibrium with entrapped air. *Nature* 405:1040–1044
- Amaral HI, Aeppli C, Kipfer R, Berg M (2011) Assessing the transformation of chlorinated ethenes in aquifers with limited potential natural attenuation: added values of compound-specific carbon isotope analysis and groundwater dating. *Chemosphere* 85:774–781
- Ayraud V, Aquilina L, Labasque T, Pauwels H, Molenat J, Pierson-Wickmann AC, Durand V, Bour O, Tarits C, Le Corre P, Fourre E, Merot P, Davy P (2008) Compartmentalization of physical and chemical properties in hard-rock aquifers deduced from chemical and groundwater age analyses. *Appl Geochem* 23(9):2686–2707
- Baek W, Lee J (2011) Source apportionment of trichloroethylene in groundwater of industrial complex in Wonju, Korea: a 15-year dispute and perspective. *Water Environ J* 25(3):336–344
- Beneteau KM, Aravena R, Frappe SK (1999) Isotopic characterization of chlorinated solvents-laboratory and field results. *Org Geochem* 30:739–753
- Böhlke JK, Denver JM (1995) Combined use of groundwater dating, chemical, and isotopic analyses to resolve the history and fate of nitrate contamination in two agricultural watersheds, Atlantic coastal plain, Maryland. *Water Resour Res* 31:2319–2339
- Burton WC, Plummer LN, Busenberg E, Lindsey BD, Gburek WJ (2002) Influence of fracture anisotropy on ground water ages and chemistry, Valley and Ridge Province, Pennsylvania. *Ground Water* 40(3):242–257
- Cey BD, Hudson GB, Moran JE, Scanlon BR (2008) Impact of artificial recharge on dissolved noble gases in groundwater in California. *Environ Sci Technol* 42:1017–1023
- Chambers JE, Wilkinson PB, Wealthall GP, Loke MH, Dearden R, Wilson R, Alen D, Ogilvy (2010) Hydrogeophysical imaging of deposit heterogeneity and groundwater chemistry changes during DNAPL source zone bioremediation. *J Contam Hydrol* 118:43–61
- Cook PG, Böhlke JK (2000) Determining timescales for groundwater flow and solute transport. In: Cook PG, Herczeg AL (eds) *Environmental tracers in subsurface hydrology*. Kluwer, Boston, pp 1–30
- Gangwon Province (2005) Detailed investigation and basic remediation design for contaminated soil and groundwater in the Woosan Industrial Complex, Wonju City, Gangwon Province, Korea
- Gourey L, Baran N, Benoit V (2009) Improving the knowledge of pesticide and nitrate transfer process using age-dating tools (CFC, SF₆, ^3H) in a volcanic island (Martinique, French West Indies). *J Contam Hydrol* 108:107–117
- Holocher J, Matta V, Aeschbach-Hertig W, Beyerle U, Hofer M, Peters F, Kipfer R (2001) Noble gas and major element constraints on the water dynamics in an alpine floodplain. *Ground Water* 39:841–852
- Jeong C, Kim K, Nagao K (2012) Hydrogeochemistry and origin of CO₂ and noble gases in the Dalki carbonate waters of the Chungsong area. *J Eng Geol* 22:123–134
- Kaown D, Koh D-C, Lee K (2009) Effects of groundwater residence time and recharge rate on nitrate contamination deduced from $\delta^{18}\text{O}$, δD , $^3\text{H}/^3\text{He}$ and CFCs in a small agricultural area in Chuncheon Korea. *J Hydrol* 366:101–111
- Kaown D, Shouakar-Stash O, Yang J, Hyun Y, Lee K (2013) Identification of multiple sources of groundwater contamination by dual isotopes. *Groundwater*. doi:10.1111/gwat.12130
- Klump S, Kiper R, Cirpka O, Harvey C, Brennwald M, Ashfaq KN, Badruzzaman AB, Hug SJ, Imboden DM (2006) Groundwater dynamics and arsenic mobilization in Bangladesh assessing using noble gases and tritium. *Environ Sci Technol* 40:243–250
- Koh D-C, Chae G-K (2008) Estimation of mixing properties and mean residence time using ^3H for groundwater in typical geothermal and CO₂-rich areas in South Korea. *J Geol Soc Korea* 44(4):507–522
- Koh D-C, Mayer B, Lee K-S, Ko K-S (2010) Land-use controls on sources and fate of nitrate in shallow groundwater of an agricultural area revealed by multiple environmental tracers. *J Contam Hydrol* 118(1–2):62–78
- Korea Institute of Nuclear Safety (KINS) (2010) Environmental radioactivity survey data in Korea, vol 42. Korea Institute of Nuclear Safety, Daejeon, pp 73–74
- Lee KS, Lee CB (1999) Oxygen and hydrogen isotope composition of precipitation and river waters in South Korea. *J Geol Soc Korea* 35(1):73–84
- Lee J, Jung B, Kim J, Ko K, Chang H (2011) Determination of groundwater flow regimes in underground storage caverns using tritium and helium isotopes. *Environ Earth Sci* 63:763–770
- Luciano A, Viotti P, Papini MP (2010) Laboratory investigation of DNAPL migration in porous media. *J Hazard Mater* 176:1006–1017
- Mamyrin BA, Tolstikhin IN (1984) Helium isotopes in nature. Elsevier, Amsterdam, 273 pp
- Manning AH, Caine JS (2007) Groundwater noble gas, age, and temperature signatures in an Alpine watershed: valuable tools in conceptual model development. *Water Resour Res*. doi:10.1029/2006WR005349
- Manning AH, Solomon DK, Thiros SA (2005) $^3\text{H}/^3\text{He}$ age data in assessing the susceptibility of wells to contamination. *Ground Water* 43:353–367
- Morrison RD (2000) Application of forensic techniques for age dating and source identification in environmental litigation. *Environ Forensic* 1:131–153
- Murphy S, Ouelton T, Balard J, Lefebvre R, Clark I (2011) Tritium-helium groundwater age used to constrain a groundwater flow model of a valley-fill aquifer contaminated with trichloroethylene (Quebec, Canada). *Hydrogeol J* 19:195–207
- Park Y, Jeong J, Eom S, Jeong U (2011) Optimal management design of a pump and treat system at the industrial complex in Wonju, Korea. *J Geosci* 15:207–223
- Peeters F, Beyerle U, Aeschbach-Hertig W, Holocher J, Brennwald MS, Kipfer R (2002) Improving noble gas based paleoclimate reconstruction and groundwater dating using $^{20}\text{Ne}/^{22}\text{Ne}$ ratios. *Geochim Cosmochim Acta* 67:587–600
- Rivett MO, Clark L (2007) A quest to locate sites described in the world’s first publication on trichloroethene contamination of groundwater. *Q J Eng Geol Hydrogeol* 40:241–249
- Shapiro SD, Rowe G, Schlosser P, Ludin A, Stute M (1998) Tritium-helium 3 dating under complex conditions in hydraulically stressed areas of a buried-valley aquifer. *Water Resour Res* 34:1165–1180

- Shouakar-Stash O, Frappe S, Drimmie R (2003) Stable hydrogen, carbon, and chlorine isotope measurements of selected chlorinated organic solvents. *J Contam Hydrol* 60:211–228
- Solomon DK, Poreda RJ, Cook PG, Hunt A (1995) Site characterization using $^3\text{H}/^3\text{He}$ ground-water ages, Cape Cod, MA. *Ground Water* 33(6):988–996
- Squillace PJ, Moran MJ, Price CV (2004) VOCs in shallow groundwater in new residential/commercial area of United States. *Environ Sci Technol* 38:5327–5338
- Sturchio NC, Clausen LJ, Huang L, Holt BD, Abrajano JR (1998) Chlorine isotope investigation of natural attenuation of trichloroethene in an aerobic aquifer. *Environ Sci Technol* 32:3037–3042
- Visser A, Broers HP, Bierkens MFP (2007) Dating degassed groundwater with $^3\text{H}/^3\text{He}$. *Water Resour Res* 43(10):WR10434. doi:10.1029/2006WR005847
- Visser A, Schaap JD, Broers HP, Bierkens MFP (2009) Degassing of $^3\text{H}/^3\text{He}$, CFCs and SF_6 by denitrification: measurements and two-phase transport simulations. *J Contam Hydrol* 103(3–4):206–218. doi:10.1016/j.jconhyd.2008.10.013
- Yang J, Lee K (2012) Locating plume sources of multiple chlorinated contaminants in groundwater by analyzing seasonal hydrological responses in an industrial complex, Wonju, Korea. *J Geosci* 16:301–311
- Yoon YY, Cho SY, Lee CK, Kim Y (2007) Low level tritium analysis using liquid scintillation counter. *Anal Sci Tech* 20:419–423
- Yu S, Chae G, Jeon K, Jeong J, Park J (2006) Trichloroethylene contamination in fractured bedrock aquifer in Wonju, South Korea. *Bull Environ Contam Toxicol* 76:341–348
- Zoellmann K, Kinzelbach W, Fulda C (2001) Environmental tracer transport (^3H and SF_6) in the saturated and unsaturated zones and its use in nitrate pollution management. *J Hydrol* 240:187–205
- Zuber A (1986) Mathematical models for the interpretation of environmental radioisotopes in groundwater systems. In: Fritz P, Fontes JC (eds) *Handbook of environmental isotope geochemistry, the terrestrial environment B*, vol 2. Elsevier, New York, pp 1–59